

Comparison of Binding Energy of Methane with Calcium Benzene Dication Complex ion $[\text{Ca}(\text{Benzene})_2]^{2+}$ on DFT and PEC in the Gas Phase

Joseph K. Koka

School of Chemistry, University of Nottingham, University Park, Nottingham NG7 2RD, United Kingdom.

School of Physical Science, Department of Chemistry, University of Cape Coast, Ghana.

ARTICLE INFO

Article history:

Received: 08 December 2018;

Received in revised form:

01 January 2019;

Accepted: 10 January 2019;

Keywords

Binding Energy,

Methane,

Benzene,

Calcium,

Density Function Theory,

Potential Energy Curve,

Gas Phase,

Complex Ion.

ABSTRACT

The UV photofragment spectrum of the dication sandwich complex ion $\text{Ca}(\text{Benzene})_2]^{2+}$ had been recorded in the gas phase using a quadrupole ion trap mass spectrometer. From the DFT calculations, the optimised C_2 and C_{2v} conformers of $\text{Ca}(\text{Benzene})_2]^{2+}$ were confirmed. Methane activation with calcium benzene dication complex ion resulted in the formation of methane calcium benzene dication complex ion $[\text{Ca}(\text{Benzene})_2\text{CH}_4]^{2+}$ and methane calcium benzene mono-cation $[\text{Ca}(\text{Benzene})\text{CH}_4]^+$. The calculated charge on the metal centre was reduced by 40% in the optimised geometry of $[\text{Ca}(\text{Benzene})_2\text{CH}_4]^{2+}$ as compared to the charge of +2 assumed on Ca metal in the potential energy curve, (PEC) calculation. The DFT calculated result revealed that the binding energy of methane to the metal dication complex ion was 13.28% lower compare to the value obtained on the PEC model.

© 2019 Elixir All rights reserved.

Introduction

Methane is an unavoidable by-product of our lifestyle [1]. During the production and transport of coal, natural gas and oil methane is emitted. Other sources of methane emission include from livestock and other agricultural practices, by the decay of organic waste in municipal solid waste landfill [2]. The very large reserves of methane, could serve as a feedstock for the production of chemicals and as a source of energy well into the 21st century. Approximately 60% globally of total methane emissions come from human activities such as agricultural, coal mining, landfills, natural gas and oil activities, and the rest are from natural resources [3]. Methane and carbon dioxide like other greenhouse gases can trap heat in the atmosphere, although methane present in the atmosphere is very low compared to CO_2 , is 21 times more potent per unit as a greenhouse gas. Since 2006 the concentration of methane in the atmosphere has risen sharply by about 25 teragrams per year [4]. In 2016, methane accounted for about 10 percent of all U.S. greenhouse gas emissions from human activities [2]. Currently methane is being used in such important applications as the heating of homes and the generation of hydrogen for ammonia synthesis. However, is a greatly underutilized resource for chemicals and liquid fuels [6]. The target of the 21st century is to keep the increase of global warming less than 2°C [5] and this could partly be achieved if methane could be converted to useful product such as methanol.

A key feedstock for the production of chemicals is methanol, some products such as plastics, plywood and paints could be made from methanol [7]. Methanol is widely regarded as a promising alternate for automobile fuel hence introduction of transportation of vehicles that are able to burn pure methanol or blended methanol would be of high

beneficial as per the environment and energy considerations [8]. The advantages of developing a world-wide market for methanol as fuel are: (i) over dependency on foreign source of energy would be reduced. (ii) the existing petroleum based energy reserves would be conserved. (iii) less demand for petroleum-based fuels leading to reducing in prices and (iv) friendly environment due to improved emissions intrinsic in combustion of methanol as compared to petroleum-based fuels. Additionally, embracing of methanol as a primary automobile or transportation fuel would compel a large increase in the world's methanol production capacity. This would make methane a much more attractive and value energy source which is easily transportable as compared to its origin [8]. Methanol also can fuel vehicles or be reformed to produce high-grade hydrogen for fuel cells [9].

Like the transition metal ions the UV-visible spectra of alkaline earth metal complexes are routinely recorded in the condensed phase either in solution or in the form of a matrix [10,11], hence they face similar experimental challenges of inhomogeneous broadening and perturbation of the spectra due to the presence of solvent molecules and counterions introduced. Gas-phase spectroscopy, in contrast, has the advantage of permitting the research of isolated species independently void of solvent molecules and counterions interference. In addition the difficulties encountered with the preparation and/or instability of a given type of complex in studies of condensed phase which may impede any systematic survey of metal-ligand interactions are overcome [12]. With the formation of sufficient number densities; metal complexes can be investigated via photodissociation or photodepletion methods with infrared multiphoton excitation technology to generate vibrational spectra [13] or single photon UV-visible excitation to create electronic spectra [14].

A significant success has been made into the investigating of the interaction of alkaline earth metal ions and benzene. For instance Williams *et al* by the application of electrospray ionization Fourier-transform mass spectrometry investigated into the gas-phase reactions of hydrated divalent alkaline earth metal ions (Mg^{2+} , Ca^{2+} , Sr^{2+} and Ba^{2+}) and benzene [15].

Recently, Stace *et al* recorded the UV photo fragmentation spectra of $[Ca(Pyridine)_4]^{2+}$, $[Ca(Picoline)_4]^{2+}$ [16] and $[Ca(Benzene)_2]^{2+}$ [17] in the gas phase, using the pick-up technology with a cold ion trap mass spectrometer. Despite these successes, literature review revealed that no work was done on activation of methane by calcium benzene dication complex ion in the gas phase. This research sought to activate methane by $[Ca(Benzene)_2]^{2+}$ in the gas phase using the pick-up technology. Successful activation of methane can serve as feedstock for a vast variety of significant industrial processes. Fancy, a small plant that has methane as input where resources of methane could be used much more efficiently. For instance, partial oxidation of methane provides a single route of direct converting of methane to liquid methanol as shown by the equation $CH_4 + \frac{1}{2}O_2 \rightarrow CH_3OH$

Experimental section

$[Ca(Benzene)_2]^{2+}$ ions were synthesised in the gas phase and their spectra recorded via UV photofragment spectroscopy within an ion trap mass spectrometer cooled to between 100-150 K. A schematic diagram of the apparatus is shown in Figure 1.

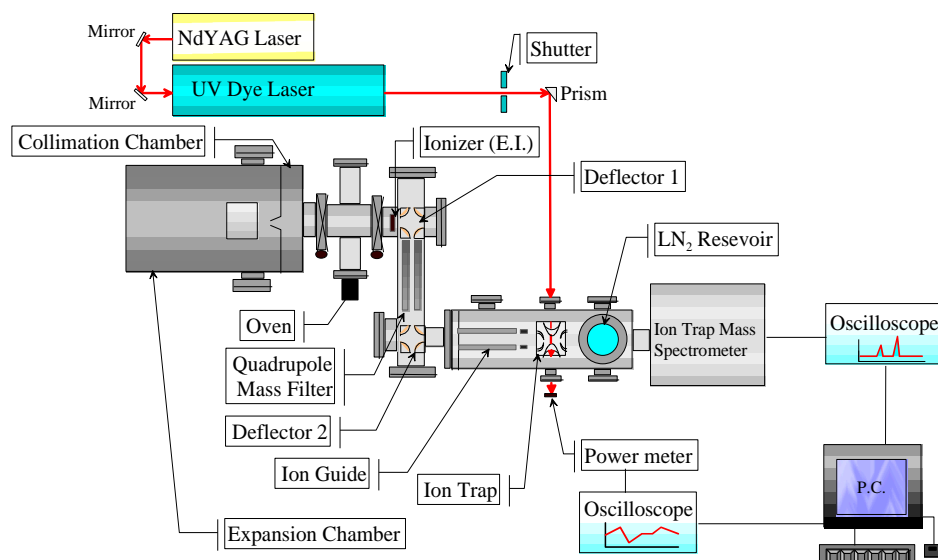


Figure 1. The diagram illustrating the experimental set up.

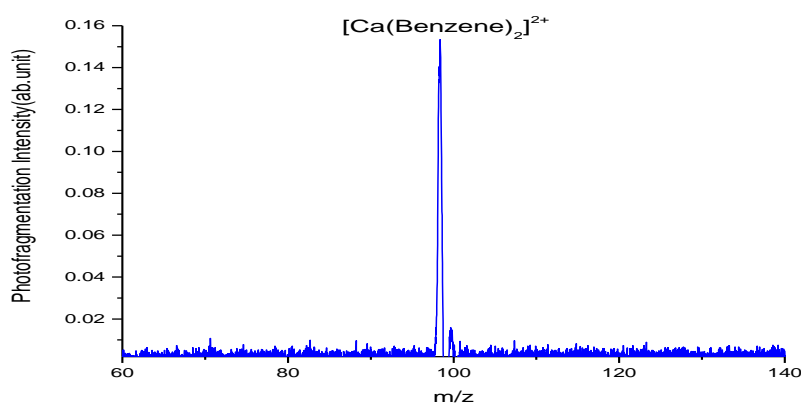


Figure 2. Mass spectra of calcium dication-benzene complex.

Neutral $[Ca(Benzene)_2]^{2+}$ clusters were generated via the pickup technique [18], whereby argon carrier gas at a pressure of 130 psi was passed through a reservoir of benzene held at room temperature. The resultant mixture, containing approximately 1% benzene vapour, underwent supersonic expansion through a 50mm diameter nozzle before passing through a 1 mm diameter skimmer.

The emerging beam of mixed argon/ benzene clusters then passed over the top of a Knudsen cell containing calcium chips heated to 590°C, which was sufficient to generate a metal vapour pressure of 10^{-3} to 10^{-2} mbar. Collisions between metal vapour and the mixed clusters generated neutral metal-containing clusters, which were then ionised by high energy electron impact (100 eV) in the ion source of a quadrupole mass spectrometer (Extrel). From the mixture a doubly charged ions (Figure 2), $[Ca(Benzene)_2]^{2+}$ was mass selected and directed by an ion guide into a Paul ion trap. The end caps of the latter were grounded and continuously cooled through direct contact with a liquid nitrogen reservoir. As a consequence, helium buffer gas (5×10^{-4} mbar) contained within the trap was also cooled and over a total trapping time of 1s, collisions between the helium and trapped ions led to a considerable reduction in the internal energy content of the latter [19]. Based on the observation of unimolecular decay by trapped ions, the internal temperature was thought to drop from 4500 K to somewhere in the range 100–150 K. This cooling procedure has led to the appearance of discrete structure in the spectra.

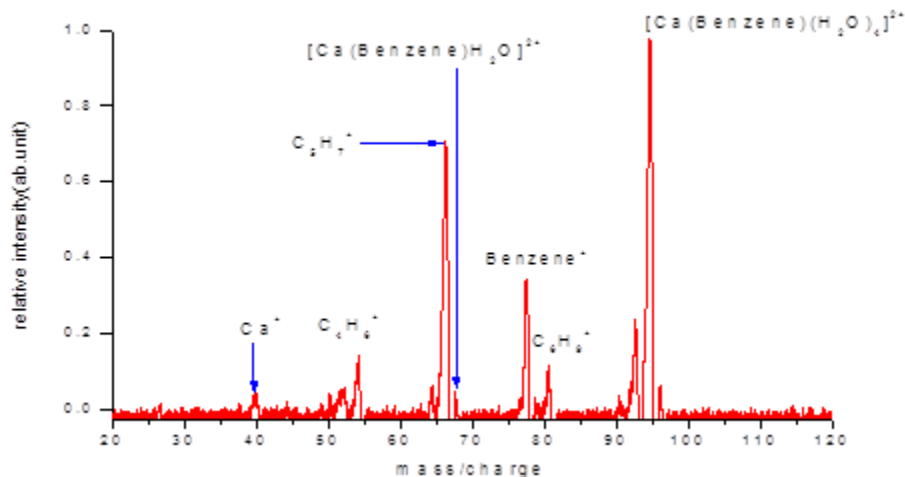


Figure 3. UV photofragment mass spectrum of calcium dication-benzene complex (wave number=38610 cm^{-1}).

The experimental apparatus could be run as a quadrupole mass spectrometer; Figure 2 shows the mass spectrum of the ion beam showing the formation of clusters with a mass/charge ratio of between 60 and 140 based on the mass spectrometer's preset calibration. The ion optics were tuned to maximise the signal of the desire $[\text{Ca}(\text{Benzene})_2]^{2+}$ dication complex ion, which would amplify peak heights around the metal complex at 98 amu.

Nonetheless, this current mass spectrum sharply contradicts the previous result where the parent ion was observed at 95 amu [17] which equates to $[\text{Ca}(\text{benzene})(\text{H}_2\text{O})_4]^{2+}$, instead of the expected $[\text{Ca}(\text{Benzene})_2]^{2+}$ at 98 amu. The exact peak position of the parent calcium benzene dication complex ion $[\text{Ca}(\text{Benzene})_2]^{2+}$ at 98 amu recorded in this current research is probably due to improve efficiency of the ion trap. From Table 1 the $[\text{Ca}(\text{Benzene})_2]^{2+}$ ion peak should be observed in the trap since the calculated binding energy of calcium benzene dication complex ion is high enough to form a stable complex ion $[\text{Ca}(\text{Benzene})_2]^{2+}$ in the ion trap.

Figure 3 represents a typical photofragmentation mass spectrum recorded under the laser radiation of photon energy of 38610 cm^{-1} . The ability of the parent calcium benzene dication complex ion to photodissociate is demonstrated by the disappearance of the parent calcium benzene dication complex ion at 98 amu. The resultant effect was photofragmentation route of benzene yielding the daughter ion $[\text{Ca}(\text{Benzene})]^{2+}$; which picks water molecule(s) to form the mono hydrated and tetrahydrated calcium mono benzene dication complex ions $[(\text{Ca}(\text{Benzene})\text{H}_2\text{O})]^{2+}$ at 68 amu and $[(\text{Ca}(\text{Benzene})(\text{H}_2\text{O})_4)]^{2+}$ at 95 amu respectively.

The ion peaks recorded at 40 and 79 amu suggest two strong routes of the daughter photofragment ion $[\text{Ca}(\text{Benzene})]^{2+}$ to further photodissociate to form photofragments Ca^+ at 40 amu and benzeneH^+ at 79 amu.

The photofragmentation of $[(\text{Ca}(\text{Benzene})_2)]^{2+}$ to form the daughter photofragment of $[(\text{Ca}(\text{Benzene}))]^{2+}$ suggests the loss of benzene as photofragmentation route. Undoubtedly the benzene molecule undergo further photodissociation to form the ion peaks of C_4H_6^+ at 54 amu, C_5H_7^+ at 67 amu and C_6H_9^+ at 81 amu similar to what has been observed previously [17]. The benzene^+ fragmentation possibly arises from either by electron impact in the ion source or collision between benzene and other molecules (such as helium) in the ion trap. The strong affinity of $[(\text{Ca}(\text{Benzene}))]^{2+}$ complex ion for water is demonstrated by the tetrahydrated calcium benzene dication complex ion formed.

Theory

The density functional theory as implemented in GAUSSIAN 09 [20] was used to calculate structures and binding energies of $[\text{Ca}(\text{benzene})_2]^{2+}$ and complex ions with methane. The local density approximation (LDA) [21] together with the gradient-corrected exchange of Becke [22] and the correlation correction of Perdew [23] (BVP86) were applied on geometry optimization and frequency analysis. Structural minima were verified by the absence of imaginary vibrational modes. These calculations were compared with results calculated using the metahybrid functional of Tao, Perdew, Staroverov, and Scuseria (TPSSH) [24]. All energies presented are zero point energy corrected.

The staggered and eclipsed parallel structures of the $[\text{Ca}(\text{Benzene})_2]^{2+}$ complex, with symmetries D_{6d} and D_{6h} , respectively, are stationary states, characterized by a large imaginary mode. When distorted, results in the bent hemi-directed geometries analogues, with symmetries C_2 (staggered) and C_{2v} (eclipsed), respectively. In both cases of a centroid-Ca-centroid angle of 180° distorted to approximately 171°C ,

Calculated Structures And Binding Energies of $[\text{Ca}(\text{BENZENE})_2]^{2+}$

Table 1. Binding Energies for the Ca^{2+} Complexes with respect to various Products formed and Calculated using both BVP86/6311++G(d,p) and TPSSH/6311++G(d, p).

Reaction	STRUCTURE	Energy / kJmol^{-1}	
		BVP86	TPSS
$[\text{CaBz}_2]^{2+} \rightarrow \text{Ca}^{2+} + 2\text{Bz}$	C2v: Eclipsed	561.29	561.00
	C2: Staggered	561.30	561.10
$[\text{Ca}(\text{Bz})_2]^{2+} \rightarrow [\text{Ca}(\text{Bz})]^+ + (\text{Bz})^+$	C2v: Eclipsed	166.00	166.00
	C2: Staggered	166.20	166.10
$[\text{Ca}(\text{Bz})_2]^{2+} \rightarrow [\text{CaBz}]^{2+} + \text{Bz}$	C2v:Eclipsed	200.00	200.00
	C2:Staggered	200.10	200.10
$\text{CaBz}_2(\text{CH}_4)^{2+} \rightarrow [\text{CaBz}_2]^{2+} + \text{CH}_4$		27.26	27.26

Activation of Methane by Calcium Benzene Diction Complex Ions

The introduction of methane into the trap (Figure 4) and irradiated under laser power revealed a series of peaks. The parent ion peak observed at $[\text{Ca}(\text{Benzene})_2]^{2+}$ at 98 amu and the parent picking a molecule of methane to form the methane calcium benzene dication complex ion of $[\text{Ca}(\text{Benzene})_2(\text{CH}_4)]^{2+}$ was observed at a peak of 106 amu. The photofragmentation loss of benzene^+ of ion peak observed at 77 amu has experienced approximately 98.6% decline in ion peak intensity as compared to the ion peak intensity in Figure 3.

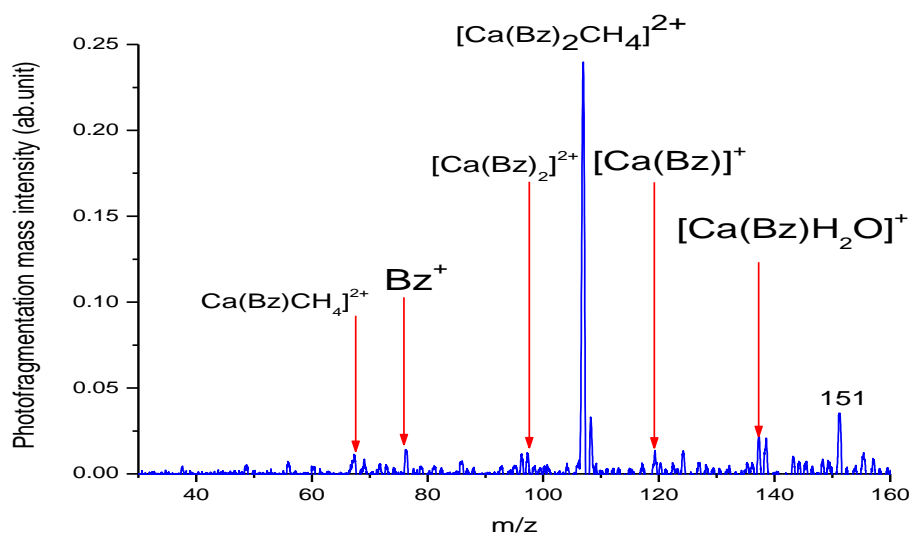


Figure 4. Photofragment mass spectrum of $[\text{Ca}(\text{Benzene})_2\text{CH}_4]^{2+}$ (Photon energy = 44000 cm^{-1}).

However, a daughter ion peak of calcium benzene mono cation complex ion $[\text{Ca}(\text{Benzene})]^{+}$ due to the photo fragmentation loss of benzene⁺ was identified and recorded at 118 amu. The ability of the coordinatively unsaturated $[\text{Ca}(\text{Benzene})]^{+}$ to pick up a water molecule to form the hydrated calcium benzene mono cation complex ion $[\text{Ca}(\text{Benzene})(\text{H}_2\text{O})]^{+}$ was recorded at the ion peak position at 136 amu.

The loss of benzene was observed resulting in the formation of a major fragment peak corresponding to coordinatively unsaturated calcium monobenzene dication complex ion $[\text{Ca}(\text{Benzene})]^{2+}$ picking up methane to form methane calcium monobenzene dication complex ion $[\text{Ca}(\text{Benzene})\text{CH}_4]^{2+}$ at 67 amu.

The Optimized Geometry of $[\text{Ca}(\text{BENZENE})_2\text{CH}_4]^{2+}$

At the optimised geometry of $[\text{Ca}(\text{Benzene})_2\text{CH}_4]^{2+}$ the initial centroid-ca-centroid bond of 180° is distorted drastically to 144.05° (Figure 5), while the initial hydrogen-carbon-hydrogen bonds in methane also experience distortion from 109.5° to between 105.26° and 112.80° .

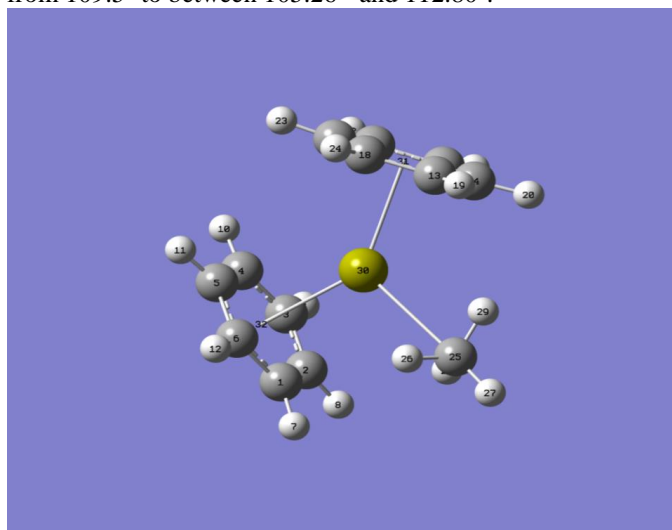


Figure 5. The Optimized geometry of $[\text{Ca}(\text{BENZENE})_2\text{CH}_4]^{2+}$ with C_1 Symmetry. The One Dimensional Potential Energy Curve of $[\text{Ca}(\text{BENZENE})_2\text{CH}_4]^{2+}$

In order to represent the observed charge separation reaction qualitatively, a one dimensional potential energy curve (PEC) model was plotted as detailed in Figure 6. From

the curves, it could be seen that the photo induced charge transfer to give $\text{Ca}(\text{Benzene})^{+}$ and CH_4^{+} of $[\text{Ca}(\text{Benzene})_2\text{CH}_4]^{2+}$ was not observed because this reaction is endothermic as evidenced by observing that the repulsive energy curve (red) lies above the attractive curve (blue).

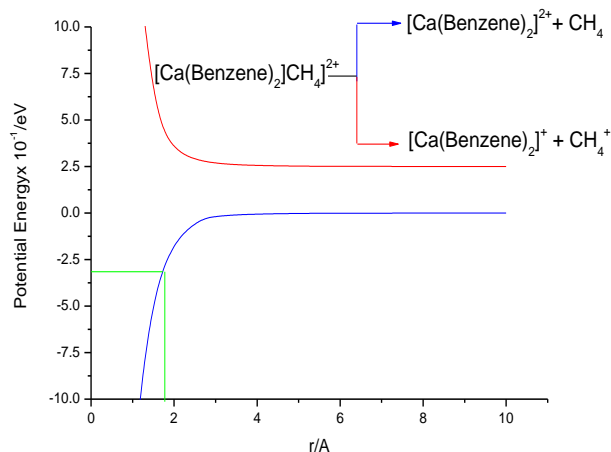


Figure 6. The potential energy surface curve model showing attractive curve and repulsive of ion-ligand $[\text{Ca}(\text{Benzene})_2\text{CH}_4]^{2+}$.

At the optimised geometry of $[\text{Ca}(\text{Benzene})_2\text{CH}_4]^{2+}$ the calcium-methane (Ca-C) distance was observed to be approximately 1.80 \AA which corresponded to 0.32 eV (30.88 kJ/mol) on the PEC model resulting in a difference of 3.62 kJ/mol higher in energy than DFT calculated value of 27.26 kJ/mol . This energy difference was evidenced by the fact that the calculated charge on the metal centre of Ca = 1.21 in the optimised DFT geometry of $[\text{Ca}(\text{Benzene})_2\text{CH}_4]^{2+}$ while a charge of Ca = 2 was applied in the PEC model calculation.

Conclusion

The UV photofragment spectrum of the dication sandwich complex $\text{Ca}(\text{Benzene})_2]^{2+}$ had been recorded in the gas phase using a quadrupole ion trap mass spectrometer. Unlike the previous work [17] the parent ion peak of $[\text{Ca}(\text{Benzene})_2]^{2+}$ was trapped and identified. From the DFT calculations, the optimised C_2 and C_{2v} conformers of $\text{Ca}(\text{Benzene})_2]^{2+}$ were confirmed. Activation of methane with calcium benzene dication complex ion resulted in the formation of methane calcium benzene dication ion

$[\text{Ca}(\text{Benzene})_2\text{CH}_4]^{2+}$ and methane calcium benzene monocation $[\text{Ca}(\text{Benzene})\text{CH}_4]^+$. The calculated charge on the metal centre was reduced by 40% in the optimised geometry of $[\text{Ca}(\text{Benzene})_2\text{CH}_4]^{2+}$ as compared to the charge of +2 assumed on Ca metal in the PEC calculation. The DFT calculated value showed that the binding energy of methane to the metal dication complex ion was 13.28% lower compared to value obtained on the PEC model. This difference could be attributed to the charge variation on the calcium metal centre in both cases.

Acknowledgement

The author would like to thank Prof. Anthony Stace of *University of Nottingham School of Chemistry, UK* for all the sacrifice, contributions and support to see this research through, Dr Lifu Ma formerly of *University of Nottingham School of Chemistry* for his contributions Prof Hazel Cox of the *University of Sussex UK*, Computational chemistry Department for the Software and computer time.

Funding

The author is indebted to British government for granting him 'International Excellence Research Award' which made the financial assistance for this research in the Nottingham University possible.

References

- [1] Tom Rickey, (2017) Cooperating microbes convert methane to alternative fuel source PNNL, (509) 375-3732 <https://www.pnnl.gov/news/release.aspx?id=4375>
- [2] United States Environmental Protection Agency (2016) Greenhouse Gas Emissions Overview of Greenhouse Gases www.epa.gov/ghgemissions/overview-greenhouse-gases
- [3] IEA (2009), Energy Sector Methane Recovery and Use, The Importance of Policy.
- [4] <https://earthobservatory.nasa.gov/images/91564/what-is-behind-rising-levels-of-methane-in-the-atmosphere>
- [5] H. K. Mohajan (2012) Dangerous Effects of Methane Gas in Atmosphere *Journal of Economic and Political Integration*, 2(1): 3–10.
- [6] J.A. Lercher, J.H. Bitter, A.G. Steghuis, J.G. Van Ommen, K. Seshan, in: F.J.J.G. Janssen, R.A. van Santen (Eds.), (1999) *Environmental Catalysis*, Imperial College Press, London, pp.103–126.
- [7] Science News (2017) Breakthrough process for directly converting methane to methanol www.sciencedaily.com/.
- [8] Priyank Khirsariya, Raju K. Mewada (2013) Single Step Oxidation of Methane to Methanol- Towards a Better Understanding. *SciVerse ScienceDirect Procedia Engineering* 51, 409 - 415.
- [9] ScienceDaily (2017) Breakthrough process for directly converting methane to methanol <https://www.sciencedaily.com/releases/2017/11/171130133831.htm>

- [10] Ma, J. C., Dougherty, D. A. (1997), The cation- π interaction. *Chem. Rev.*, 97: 1303-1324
- [11] Lever, A. B. P. (1984): *Studies in Physical and Theoretical Chemistry*, Elsevier, Amsterdam, Oxford, New York, Tokio. *Inorganic Electronic Spectroscopy*, Vol. 33 aus 863 Seiten
- [12] Cotton, F. A., Wilkinson, G., *Advanced Inorganic Chemistry*. Wiley: London, 1988.
- [13] Wu, G., Guan, J., Aitken, G. D. C., Cox, H., Stace, A. J., (2006) Infrared multiphoton spectra from metal dication complexes in the gas phase *J. Chem. Phys.*, 124. doi.org/10.1063/1.2194547
- [14] Puskar, L., Barran, P. E., Wright, R. R., Kirkwood, D. A., Stace, A. J., (2000) The ultraviolet photofragmentation of doubly charged transition metal complexes in the gas phase: Initial results for $[\text{Cu}(\text{pyridine})_n]^{2+}$ and $[\text{Ag}(\text{pyridine})_n]^{2+}$ ions *J. Chem. Phys.*, 112 7751. doi.org/10.1063/1.481381
- [15] Rodriguez-Cruz, S. E., Williams, E. R., *J. Am. Soc. Mass Spectrom* 2001, 12.
- [16] Stewart, H., Wu, G., Ma, L., Barclay, M., Vieira, A. D., King, A., Cox, H., Stace, A. J., (2011). Ultraviolet photofragmentation spectroscopy of alkaline earth dication complexes with pyridine and 4-picoline (4-methyl pyridine). *J. Phys. Chem. A*, 115. DOI:10.1021/jp112171j
- [17] Ma, L., Ultraviolet Photofragmentation Spectroscopy of Metal Dication Sandwich Complexes in the Gas Phase Combined with DFT/TDDFT calculations. PhD thesis, University of Nottingham, 2013.
- [18] A.J. Stace, (2002) Metal Ion Solvation in the Gas Phase: The Quest for Higher Oxidation States *J. Phys. Chem. A* 106, 7993 DOI: 10.1021/jp020694t
- [19] G. Wu, D. Chapman and A.J. Stace, (2007). Trapping and recording the collision- and photo-induced fragmentation patterns of multiply charged metal complexes in the gas phase *Int. J. Mass Spectrom.* 262, 211-262: 211-219. DOI: 10.1016/j.ijms.2006.11.012
- [20] M. J. Frisch, G. W. Trucks, H. B. Schlegel *et al.*, (2009) GAUSSIAN 09, Revision A.02, Gaussian, Inc., Wallingford, CT,
- [21] S. H. Vosko, L. Wilk, and M. Nusair, (1980), *Can. J. Phys.* **58**, 1200 DOI.org/10.1139/p80-159
- [22] A. D. Becke, *Phys. Rev. A* **38**, 3098 (1988), doi.org/10.1103/PhysRevA.38.3098
- [23] J. P. Perdew, *Phys. Rev. B* **33**, 8822 (1986). doi.org/10.1103/PhysRevB.33.8822
- [24] J. Tao, J. P. Perdew, V. N. Staroverov, and G. E. Scuseria, (2003). *Phys. Rev. Lett.* **91**, 146401